Pressure-temperature phase diagram of solid and liquid Te under pressures up to 10 GPa

Pressure–temperature phase diagram of solid and liquid Te under pressures up to 10 GPa

V V Brazhkin, R N Voloshin, S V Popova and A G Umnov

Institute of High Pressure Physics, USSR Academy of Sciences, 142092 Troick, Moscow Region, USSR

Abstract. The P–T phase diagram of Te has been investigated by means of thermobaro-analysis (TBA) and electrical resistance measurements. For crystalline Te the boundary of the transition Te_{III}–Te_{IV} has been found and the location of triple point Te_{III}–L'–Te_{IV} has been established ($P = 7.6 \pm 0.3$ GPa; $T = 835 \pm 15$ K). The melting curve of Te was investigated up to 10 GPa. In the Te melt the transition L–L' has been found from the TBA signal and by jumps in the electrical resistance. The triple point L–Te_{III}–L' has been found to be located at $P = 4.7 \pm 0.3$ GPa and $T = 800 \pm 15$ K. At pressures lower than $P = 1.6 \pm 0.4$ GPa and temperatures higher than $T = 1120 \pm 30$ K the TBA anomalies and the jumps in resistance become smooth and unmeasurable.

The model of a phase transition in a liquid is presented based on the existence of crystal-like clusters in the melt.

1. Introduction

In recent years the phase transitions in melted substances have been actively investigated [1–4]. In [2] the data on changes in short-range order structure in Bi, Ce and Cs melts under pressure were presented. In Se and Bi [3, 4] these transitions are established as rather sharp and accompanied by volume and electrical resistance jumps and by thermal effects, i.e. they have some features of first-order phase transitions. At high temperatures the transitions in melts seem to have critical points [3, 4].

In crystalline Te the transitions Te_I–Te_{II} and Te_{II}–Te_{III} have been established [5] (figure 1). The transition Te_{III}–Te_{IV} was investigated only at normal temperature. The transition occurs at $P \simeq 11$ GPa [6]. The phase Te_{III} has an orthorhombic structure; Te_{IV} has a β–Po structure. At $P \simeq 27$ GPa the transition Te_{IV}–Te_V occurs [6]; the phase Te_V has a BCC structure.

The melting curve of Te has been previously established up to 7 GPa [7] (figure 1). The melt of the Te has also been actively investigated. Liquid Te has a smooth transition from a semi-metallic state to a metallic state. At normal pressure the transition occurs at $T = 800$–900 K and is accompanied by a change in coordination number from 2.6 to 3 [8]. Near the melting temperature, metallization occurs at 0.3–0.4 GPa. On the melting curve a sharp change in slope was found [9]. This allows one to assume that some volume anomalies are present in the melt. Anomalies in the electrical resistance of molten Te at $P < 1.8$ GPa were found and reported in [10] (see figure 1).
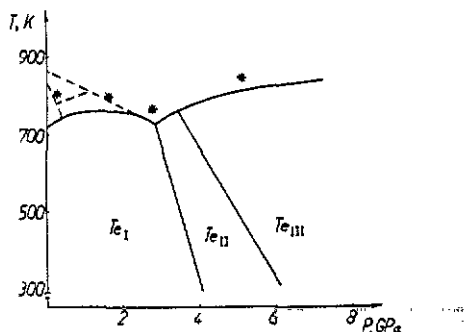
Figure 1. $P-T$ phase diagram of Te: ——— , lines separating different phases of Te from the data in [5];----, lines of electrical resistance anomalies in molten Te [10]; *, regions in which the structure factor of liquid Te was investigated [11].
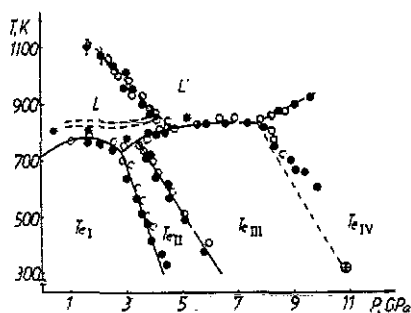
Figure 2. $P-T$ phase diagram of Te: ——— , lines of the phase diagram of Te up to 7 GPa [7]; ----, lines of equilibrium L-L′ and Te_{III}-Te_{IV} from the data in this paper; ===, weak irreproducible anomalies of TBA and resistance; O, TBA anomalies (the dimension of symbol corresponds to the width of the transition; ●, anomalies in the conductivity; ♦, width of transition near the critical point; *, regions where the structure factor was measured [11]; ⊕, Te_{III}-Te_{IV} transition in accordance with [6].

In [11] it was shown that the short-range order structure in the Te melt at $P <$ 2.6 GPa is analogous to that for the crystalline phases Te_{II} and Te_{III}, but at $P \simeq$ 5.1 GPa the structure factor differs essentially from that at $P < 2.6$ GPa.

In this paper the experimental investigation of the $P-T$ phase diagram of Te by the thermobaroanalysis (TBA) method and by the measurement of electrical resistance under pressures 1 GPa $< P <$ 10 GPa is presented.

2. Experimental details

To produce a high pressure a chamber of 'toroid' type [12] was used which has been calibrated by the well known phase transitions in Ce (0.7 GPa), Bi (2.55, 2.7 and 7.7 GPa) and Sn (9.4 GPa). The pressure-transmitting medium was pipe-stone. Heating of the samples was achieved by passing an AC through a graphite heater. The temperature was measured with chromel-alumel and Pt-(Pt-10% Rh) thermocouples. The temperature range was 300–1100 K; the heating and cooling rates were -10^{-1}–10^2 K s^{-1}. The change in pressure when a sample was heated was controlled by the TBA method using the pressure dependences of the thermocouple's EMF [13]. Volume jumps under heating were also measured by TBA anomalies [3, 4]. The accuracies of the pressure and temperature measurements were ±0.3 GPa and ±10 K, respectively.

The samples consisting of crystalline Te powder were placed in a container made of graphite or NaCl. The phase composition of the samples after an experiment was controlled by x-ray analyses (x-ray camera RKU–114; Cu Kα radiation). The heater was surrounded by a NaCl or BN cylinder (external diameter, 6 mm; internal diameter, 3 mm) to eliminate the influence of the phase transitions in the pipe-stone on the TBA signal.

Table 1. Changes in resistance at various transitions.

Transition	Pressure (GPa)	$\Delta\rho/\rho$ (%)
Te$_1$–L	2	−30
Te$_{111}$–L	3.5	10
Te$_{11}$–Te$_{111}$	3.5	−3

Table 2. Changes in volume at various transitions.

Transition	$\Delta V/V$ (%)	K (GPa)
Te$_1$–Te$_{11}$	−5	54 (Te$_{11}$)
Te$_{11}$–Te$_{111}$	−1.5	57 (Te$_{111}$)
Te$_{111}$–Te$_{1V}$	−2.5	115 (Te$_{1V}$)

The electrical resistance was measured by the voltage-to-current ratio; graphite contacts were used.

To obtain the absolute values of resistance and volume jumps, well known data on the phase transitions in Te [1,5,6] were used for calibration purposes (tables 1 and 2).

3. Results and discussion

In this paper the boundary of the Te$_{111}$–Te$_{1V}$ transition and the melting curve up to 10 GPa were established.
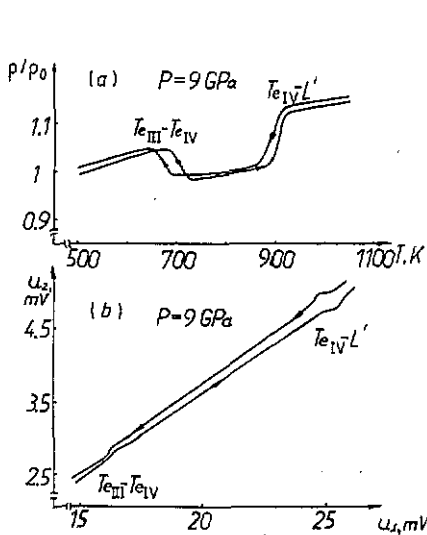

Figure 3. (a) Temperature dependence of the electrical resistance and (b) the TBA dependence during isobaric heating at $P = 9$ GPa.
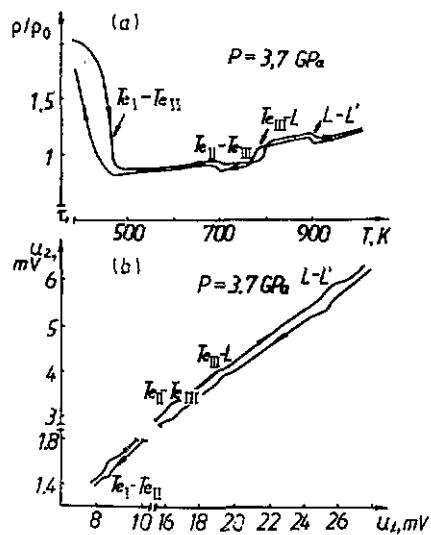
Figure 4. (a) Temperature dependence of the electrical resistance and (b) the TBA dependences during isobaric heating at $P = 3.7$ GPa.

The changes in the TBA signal and in the resistance during heating of a sample at $P = 9$ GPa are shown in figure 3. The summarized data are presented in table 3. The values of enthalpies were evaluated from the data on the values of jumps in volume and values of dT/dP for the transitions using the Clausius–Clapeyron equation.

The coordinates of the triple point Te_{III}–L'–Te_{IV} are $P = 7.6 \pm 0.3$ GPa and $T = 835 \pm 15$ K.

In molten Te the transition L–L' was found (see figure 2). The triple point Te_{III}–L–L' is located at $P = 4.7 \pm 0.3$ GPa and $T = 800 \pm 15$ K. The slope of transition L–L' is $dT/dP = -100$ K GPa^{-1}.

Table 3. Summarized data.

Transition	$\Delta \rho / \rho$ (%)	$\Delta V / V$ (%)	ΔH kJ (mol^{-1})
Te_{III}–Te_{IV}	-7 ± 2	2.5 ± 0.5	3 ± 1
Te_{IV}–L'	12 ± 1	6 ± 1	20 ± 5
L–L' near triple point	-4 ± 1	-1 ± 0.3	2 ± 0.5
Te_{III}–L ($P = 4$ GPa)	9 ± 2	5 ± 1	20 ± 4

The temperature dependences of the electrical resistance and TBA curves when a sample was being heated at constant pressure $P = 3.7$ GPa are shown in figure 4; the calculated values of $\Delta \rho / \rho$ and $\Delta V / V$ are presented in table 3.

In some experiments at $P = 1.5$–3.5 GPa and $T = 820$–920 K, weak anomalies in the TBA and resistance were obtained but these were so smooth and irreproducible that they cannot be treated as tangible phase transitions (see figure 2).

On increase in temperature, the jumps in resistance and volume at the L–L' transition decrease and at $P < 1.6$ GPa and $T > 1120$ K the jumps cannot be observed at all.

The width of the L–L' transition near the triple point is about 0.6 GPa. The change in the short-range order structure between 2.6 and 5.1 GPa described in [11] is probably connected with the transition being discussed. Our estimations based on the data in [11] on structure factor and on pressure dependence of the volume of Te [6] show the short-range order in molten Te to be based on a BCC rather than on a simple cubic lattice.

Usually structure changes in a melt are described on the basis of the two-liquid model of Rapoport [2, 14, 15], but the results in [3,4] and the data in this paper show that a transition in a liquid may appear in rather narrow pressure interval (0.5 GPa). This is in a better agreement with the model of Mitus and Patashinskii [16] where the possibility of a first-order transition in a melt is admitted. Landau and Zeldovich [17] were the first to show the possibility of a first-order phase transition in a liquid.

It is known [18] that a melt near the melting point includes long-lived crystal-like clusters. In [19] the model of a melt including only this kind of clusters is discussed and it is shown that the free energy of a quasi-gas liquid with clusters may be less than that of a 'pure' quasi-gas liquid. At the temperature $T = T^*$ the fraction x of clusters becomes zero; at melting temperature T_m, $x \simeq 10\%$ [18–20]. The number of atoms in cluster for different melts is $N_{cl} = 10$–50 [18].

Let us discuss the transition in a melt under pressure based upon the presence of clusters in a liquid.
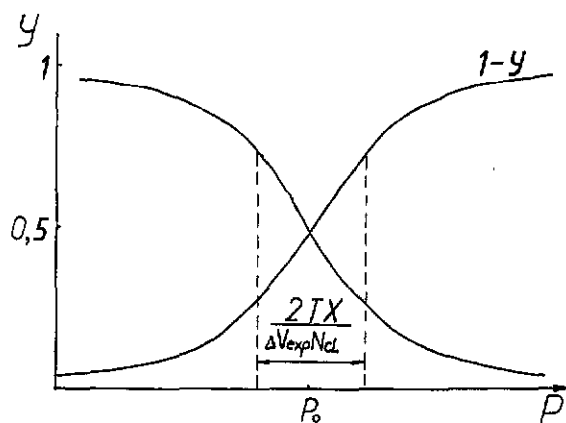
Figure 5. The change in the proportion of different clusters in the melt near transition.

Let two phases with equal chemical potentials be present in a melt at $P = P_0$. Clusters have different structure in these phases. The surrounding quasi-gas also has a different density, coordination number, etc. If the melt is a mixture of two kinds of melts, the chemical potential has an entropy addition due to mixing of different kinds of clusters. The entropy term per cluster [21] is

$$\Delta\Phi_{\text{mix}} = T[y\ln y + (1-y)\ln(1-y)]. \tag{1}$$

y is the fraction of clusters of the first kind; $1 - y$ is that of the second kind. Per atom of the melt,

$$\Delta\Phi^*_{\text{mix}} = \{Tx/[yN_{c1} + (1-y)N_{c2}]\}[y\ln y + (1-y)\ln(1-y)]. \tag{2}$$

N_{c1} is the number of atoms in a cluster of the first kind, and N_{c2} that of the second kind.

At $P = P_0 + \Delta P$, $\Delta\Phi_p$ should be added to the chemical potential because of 'PV addition'. Per atom of the melt,

$$\Delta\Phi_p = x[(y\Delta PV_1 + (1-y)\Delta PV_2]. \tag{3}$$

V_1 and V_2 are volumes per atom of the clusters of the first and second kinds, respectively, the volume of quasi-gas surrounding being considered as constant.

To summarize,

$$\Phi = \Phi_0(T, P_0) + \{Tx/[yN_{c1} + (1-y)N_{c2}]\}[y\ln y + (1-y)\ln(1-y)]$$
$$+ x[y\Delta PV_1 + (1-y)\Delta PV_2]. \tag{4}$$

Varying $\Phi(y)$ for the case $N_{c1} = N_{c2} = N_c$ one can obtain the fraction of clusters corresponding to the minimum of the chemical potential:

$$y_{\text{opt}} = 1/\{1 + \exp[(V_1 - V_2)\Delta PN_c/T]\} \tag{5}$$

i.e. at any pressure there exists a mixture of different clusters. At $P = P_0, y = \frac{1}{2}$ (figure 5).

So, the pressure dependence of the concentrations of different 'phases' of a liquid is analogous to that proposed by Rapoport but, in his model, atoms of different phases are used instead of clusters. According to this, the ΔP interval where essential alteration in the concentration of different melts takes place (say, from $\frac{1}{4}$ to $\frac{3}{4}$) using the data of Rapoport is

$$\Delta P \simeq T/(V_1 - V_2) \tag{6}$$

and from equation (5) is

$$\Delta P \simeq T/(V_1 - V_2)N_c. \tag{7}$$

So the width of the transition in our model may be in N_c times less than in the model of Rapoport. The volume and heat anomalies would take place in an interval ΔP, the values of the jumps being proportional to x (the fraction of clusters in a melt). Near T^*, x decreases to zero [19]; so T^* is a critical temperature.

On the assumption that the volume of surrounding quasi-gas also changes:

$$V^* = V_0 + x[\alpha y + \beta(1 - y)] \tag{8}$$

where V_0 is the volume per atom of surrounding quasi-gas, and α and β are constants.

In this case,

$$y_{opt} = 1/[1 + \exp\{[(V_1 - V_2) + (1 - x)(\alpha - \beta)]\Delta PN_c/T\}] \tag{9}$$

and the width of a transition is

$$\Delta P = T/[(V_1 - V_2) + (1 - x)(\alpha - \beta)]N_c = Tx/(\Delta V_{exp}N_c) \tag{10}$$

where ΔV_{exp} is the value of the experimentally observed volume jump ($\Delta V_{exp}/V$ is about 1%).

Taking, for Te, $N_c \simeq 10$–50 [18] and $x \simeq 0.1$, we obtain $\Delta P \simeq 0.2$–1 GPa near the melting temperature; hence this model does explain the small width of the transition. One can suppose that the local packing in clusters of liquid-L is based on the orthorhombic structure and liquid-L' is based on the BCC or simple cubic structure.

4. Conclusion

This paper presents the experimental data on the investigation of the P–T diagram of crystalline and molten Te by the TBA method and by resistance measurements.

In the Te melt the transition L–L' was observed and the location of the transition was established on the $(P$–$T)$ plane. One can suppose that because of this transition the change in short-range order structure in a melt takes place as was found earlier by Yaoita *et al* [11]. The transition has all the features of a first-order phase transition. The assumption of the presence of crystal-like clusters in a melt explains the narrow transition interval.

References

[1]   Endo H, Tamura K and Yao M, 1987 *Can. J. Phys.* **65** 266
[2]   Tsuji K 1990 *J. Non-Crystallogr. Solids* **117–8** 27
[3]   Brazhkin V V, Voloshin R N and Popova S V, 1989 *JETP Lett.* **50** 424
[4]   Umnov A G, Brazhkin V V, Popova S V and Voloshin R N 1991 *J. Phys.: Condens. Matter* **4** 1427
[5]   Deaton B C and Blum A C 1965 *Phys. Rev.* A **137** 1410
[6]   Parthasarathy G and Holzapfel W B 1988 *Phys. Rev.* B **37** 8499
[7]   Tonkov E 1988 *Fazovye Prevrascheniya Pri Vysokih Davleniyakh* vol 2 (Moscow: Metallurgya) p 283
        (in Russian)
[8]   Cabane B and Friedel J 1971 *J. Physique* **32** 73
[9]   Stishov S M, Tikhomirova A M and Tonkov E Yu 1966 *JETP Lett.* **4** 161
[10] Stishov S M 1967 *Sov. Phys.–JETP* **52** 1196
[11] Yaoita K, Imai M, Tsuji K, Kikegava T and Shimomura O 1991 *High Pressure Res.* at press
[12] Khvostancev L G, Vereschagin L F and Novikov A P 1977 *High Temp.–High Pressures* **2** 637
[13] Getting I C and Kennedy G C 1970 *J. Appl. Phys.* **41** 4552
[14] Rapoport E 1967 *J. Chem. Phys.* **46** 2891
[15] Rapoport E 1968 *J. Chem. Phys.* **48** 1433
[16] Mitus A S and Patashinskij A Z 1988 *Acta Phys. Pol.* **74–9** 779
[17] Landau L D and Zeldovich Ya B 1969 *Sobranie Trudov L D Landau* vol 1 (Moscow: Nauka) p 439
        (in Russian)
[18] Ubellohde A R 1978 *The Molten State of Matter* (New York: Wiley) p182
[19] Brazhkin V V 1990 *J. Non-Crystallogr. Solids* **124** 24
[20] Euring H, Ree T and Hirai N 1958 *Proc. Natl. Acad. Sci. USA* **44** 683
[21] Landau L D and Lifshits E M 1964 *Statisticheskaya Fizika* (Moscow: Nauka) p 270 (in Russian)